Dynamical reaction pathways in Eley-Rideal recombination of nitrogen from W(100)

E. Quintas-Sánchez, P. Larrégaray, C. Crespos, L. Martin-Gondre, J. Rubayo-Soneira, and J.-C. Rayez

Citation: The Journal of Chemical Physics **137**, 064709 (2012); doi: 10.1063/1.4742815
View online: http://dx.doi.org/10.1063/1.4742815
View Table of Contents: http://scitation.aip.org/content/aip/journal/jcp/137/6?ver=pdfcov
Published by the AIP Publishing

Dynamical reaction pathways in Eley-Rideal recombination of nitrogen from W(100)

E. Quintas-Sánchez,[1,2,3] P. Larrégaray,[2,3,a)] C. Crespos,[2,3] L. Martin-Gondre,[4,5]
J. Rubayo-Soneira,[1] and J.-C. Rayez[2,3]
[1]*InSTEC, Ave. Salvador Allende esq. Luaces, 10600 La Habana, Cuba*
[2]*Univ. Bordeaux, ISM, UMR 5255, F-33400 Talence, France*
[3]*CNRS, ISM, UMR 5255, F-33400 Talence, France*
[4]*Centro de Fisica de Materiales CFM/MPC (CSIS-UPV/EHU), P. Manuel de Lardizabal 4, 20018 San Sebastian, Spain*
[5]*Donostia International Physics Center, P. Manuel de Lardizabal 4, 20018 San Sebastian, Spain*

(Received 5 June 2012; accepted 24 July 2012; published online 14 August 2012)

The scattering of atomic nitrogen over a N-pre-adsorbed W(100) surface is theoretically described in the case of normal incidence off a single adsorbate. Dynamical reaction mechanisms, in particular Eley-Rideal (ER) abstraction, are scrutinized in the 0.1–3.0 eV collision energy range and the influence of temperature on reactivity is considered between 300 and 1500 K. Dynamics simulations suggest that, though non-activated reaction pathways exist, the abstraction process exhibits a significant collision energy threshold (0.5 eV). Such a feature, which has not been reported so far in the literature, is the consequence of a repulsive interaction between the impinging and the pre-adsorbed nitrogens along with a strong attraction towards the tungsten atoms. Above threshold, the cross section for ER reaction is found one order of magnitude lower than the one for hot-atoms formation. The abstraction process involves the collision of the impinging atom with the surface prior to reaction but temperature effects, when modeled via a generalized Langevin oscillator model, do not affect significantly reactivity. © *2012 American Institute of Physics*. [http://dx.doi.org/10.1063/1.4742815]

I. INTRODUCTION

The adsorption and desorption of gas-phase atoms/molecules as well as their recombination on surfaces are decisive processes in the chemistry of atmospheric[1,2] and interstellar media,[3,4] the behavior of thermal shields facing plasma—spacecrafts[5] and internal partitions of tokamaks[6,7]—the treatment of fuel combustion residuals[5] and the heterogeneous catalysis industry.[8–10]

From the theoretical point of view, molecular dynamics simulations have been widely used in the last decades to help rationalizing such elementary processes.[11] In particular, the interaction of N_2 molecules with tungsten has attracted interest[12–23] as a benchmark system for heterogeneous reactivity of heavy diatomic molecules. N_2 scattering on metals, a key step in ammonia synthesis,[8,10] leads to strong surface crystallographic anisotropies in the case of tungsten.[12,13,17,21–23] Consequently, dissociative adsorption and inelastic scattering of N_2 diatoms on surfaces of different crystallographic orientations have been extensively studied, both theoretically[15,16,18–23] and experimentally.[24–28] Besides this fundamental aspect, N_2/W reactivity is of renewed technological interest within the context of nuclear fusion.[29–31] Due to the strong interaction of nitrogen atom with tungsten surfaces, about 7.4 eV for W(100),[15] Langmuir-Hinshelwood (LH) (Refs. 9 and 32) recombination is largely endothermic by more than 4.8 eV and thus expected to play a minor role up to high temperatures.[33] On the opposite, Eley-Rideal (ER) reactions,[9,32] for which molecular formation results from direct abstraction of one (thermalized) adatom by one atom originating from the gas-phase, are significantly exothermic by about 2.4 eV (Refs. 15 and 16) and may consequently occur when the density of gas-phase atoms is non negligible, e.g., in low temperature plasma.[34] Nevertheless, to the best of our knowledge, N_2 abstraction from tungsten surfaces has not been studied neither theoretically nor experimentally so far.

Though theoretically proposed in the late 1940s,[35–37] such ER processes, characterized by sub-picosecond reaction times and highly excited products, have only been evidenced experimentally in the 1990s, within the framework of H_2 recombination on metals.[38–40] They usually lead to small cross sections and molecular recombination is primarily governed by hot atom (HA) mechanisms.[34,41–54] In HA reactions,[34,55] the gas-phase atom transfers part of its collision energy to one adsorbate and/or the metallic surface upon initial collision and is subsequently deflected towards a motion mostly parallel to the surface. Consequently, depending on surface coverage, such a hot species may react with another adatom before being thermalized. Depending on the competition between recombination and thermalization, HA reactions are characterized by dynamical features similar to ER (short reaction times) or LH (infinite reactions times) processes. Within the framework of H_2 recombination on metals, the HA channel is usually more probable than the ER one by about one order of magnitude.[50,51,53,56] In this work, we theoretically study the dynamics of ER recombination and HA formation upon scattering of a nitrogen atom under normal incidence off a single adsorbate within the framework

a)p.larregaray@ism.u-bordeaux1.fr.

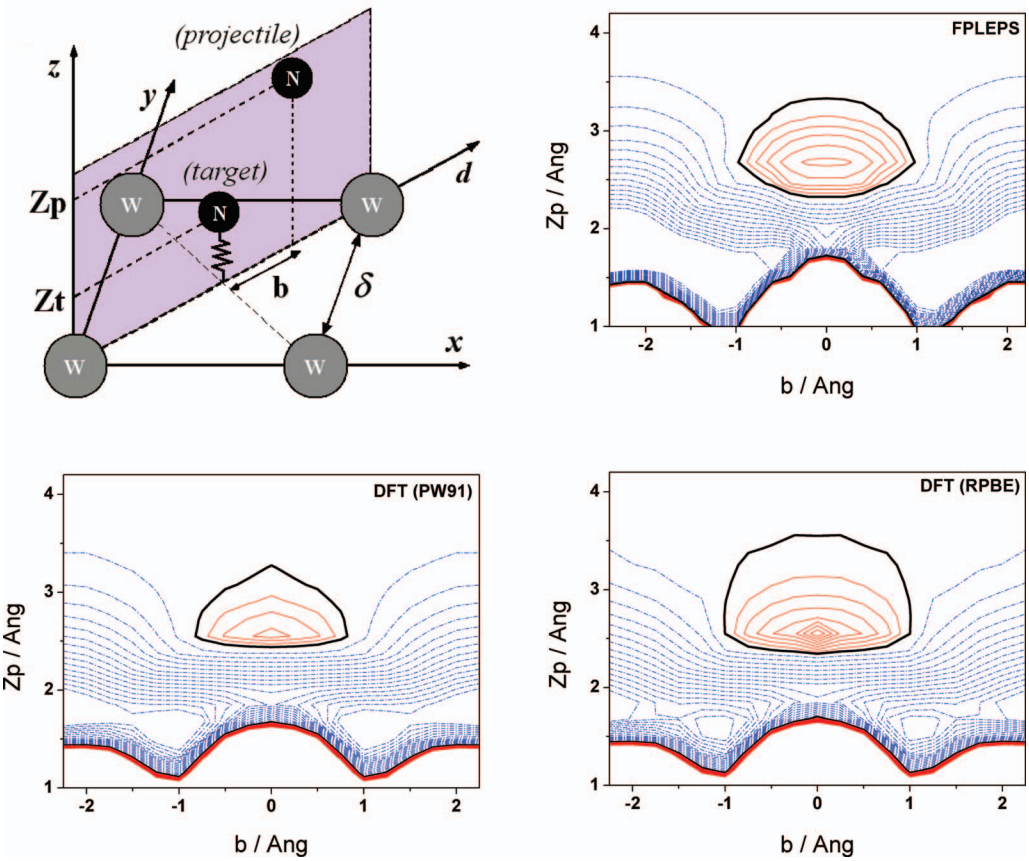

FIG. 1. Top left: Coordinate system and W(100) unitary cell. The Cartesian reference frame is originated on a tungsten top surface atom (grey circles). Black circles represent nitrogen atoms. The plane perpendicular to the surface and containing the diagonal of the unit cell is highlighted. Top right and bottom: 2D cuts of the PES as a function of projectile altitude (Zp) and impact parameter (b) within the diagonal plane. The FPLEPS model and DFT (PW91,RPBE) calculations are compared. The thick black line indicates the zero energy level, taken as the N atom adsorption energy. Full lines (dashed lines) are positive (negative) isovalues, separated by 0.1 eV (0.2 eV), $\delta = 3.175$ Å.

of frozen and moving unreconstructed W(100) surfaces. The W(100) surface is known to undergo a structural phase transition below 200K (Refs. 57 and 58) leading to a c(2x2) zigzag surface-atoms arrangement. At higher temperatures, the unreconstructed 1x1 surface structure is observed. Such features are correctly accounted for by density functional theory (DFT) calculations.[59] In this work, we only consider the unreconstructed surface and analyze temperature effects above 200K. The study mainly focuses on the rationalization of the reaction pathways leading to N_2 and HA formation and their evolution with collision energy and surface temperature.

The paper is organized as follows. Section II presents methodological details. Sections III A and III B present and discuss the results for the rigid and non-rigid models, respectively. Finally, we summarize and conclude in Section IV.

II. METHODOLOGY

We model the normal incidence scattering of a nitrogen atom (projectile) off a single nitrogen adsorbate (target) on the W(100) surface using classical molecular dynamics. Within the frozen surface approximation, the reaction occurs in a 6-dimensional configuration space (3 degrees-of-freedom for each atom). Simulating the dynamics accounting for all the degrees-of-freedom is known to be crucial in gas-surface elementary processes.[60,61] The coordinates of both nitrogen atoms are referred in a Cartesian reference frame, originated on a tungsten top surface atom. This frame as well as the W(100) unit cell are sketched in Fig. 1 (top left). The unreconstructed W(100) surface unit cell is a square, of lattice constant $\delta = 3.175$ Å. The "z" axis is defined normal to the surface and the "x" and "y" axes lie along the square axes. The surface is considered to be infinite and periodic in the (x, y) dimensions. The plane perpendicular to the surface and containing the diagonal of the unit cell, of particular importance in the following, is highlighted in the figure.

In the last fifteen years, quasi-classical trajectory (QCT) simulations, relying on the ground adiabatic electronic state, have been extensively used to investigate elementary gas-surface reaction dynamics,[11] in particular Eley-Rideal recombinations.[41–54,62,63] For processes involving at least one hydrogen atom, such a classical scattering approach has provided results in fair agreement with quantum scattering calculations in reduced dimensionalities.[42,43,50,53,62–73] Due to the high mass of the nitrogen atoms considered in this work with respect to hydrogen, the classical approximation for atomic motions is expected to hold even better.

Within the Born-Oppenheimer approximation, the N+N/W(100) recombination process is supposed to take place on the ground adiabatic electronic state. Electron-hole

(e-h) pair excitations are thus ignored. Such non-adiabatic effects have been shown to negligibly influence the N_2 dissociation and scattering dynamics on tungsten surfaces[61,74–77] as well as N scattering and short-time adsorption dynamics on Ag(111).[78,79] Though suggested to be weak in the case of H_2 recombination on Cu(111),[80] due to the ultrafast reaction time, the influence of e-h pairs on ER dynamics has not been intensively studied to date from the theoretical point of view.

In this work, the potential energy surface (PES) is a flexible periodic London–Eyring–Polanyi–Sato potential (FPLEPS). This recently developed improved version of the LEPS potential is now able to accurately describe the scattering and dissociative adsorption of nitrogen molecules on tungsten.[21–23] Such a global PES, in which all asymptotic channels are physically correct, is so far restricted to the description of two nitrogen atoms, i.e., one adsorbate within the framework of ER abstraction (zero coverage limit). Figure 1 illustrates the topology of the FPLEPS PES (top right) in the Eley–Rideal entrance channel in comparison with DFT (Refs. 81 and 82) calculations. Two-dimensional (2D) cuts are displayed as a function of the projectile altitude (Zp) and impact parameter (b) within the above-mentionned diagonal plane, the adatom siting at its hollow adsorption site (Zt = 0.65 Å) which is found to be the lowest adsorption energy site.[16] Impact parameters are given with respect to the adsorbate equilibrium position. DFT energies are computed within the generalized gradient approximation[83–90] and using the PW91 (bottom left) and RPBE (bottom right) exchange-correlation functionals[84,91–95] and ultrasoft pseudopotentials.[96–98] The surface has been modeled by a five-layer slab. DFT computation details are given elsewhere.[16]

As evidenced in Fig. 1, the ER entrance channel involves a potential energy bump located above the adsorbate which vanishes with increasing impact parameters. The N–N interaction is thus repulsive in the medium range (2.5 Å–3.5 Å) upon approach of the projectile towards the adatom for impact parameters lower than 1.0 Å. In the *ab initio* data, this repulsion is higher when using the RPBE functional. This is consistent with other DFT calculations in which such a functional has been found to lead to more pronounced medium range barriers when compared with the PW91 one.[20] Below Zp = 2.5 Å, the interaction is highly attractive towards the tungsten top atoms. Such an interaction is greater when using the PW91. The FPLEPS 2D cut quite nicely reproduces the *ab initio* data. In particular, the topology of the ER entrance channel is qualitatively captured, with the height/extension of the bump being intermediate between the ones resulting from the use of RPBE and PW91 functionals. Given the reasonable agreement between the three PESs, the conclusions inferred in the following are expected to be at least of qualitative value.

Despite the existence of the entrance channel potential energy bump, non-activated reaction pathways exist for ER abstraction. As an illustration, a 2D cut of the PES as the function of the altitude of both the target (Zt) and projectile (Zp) is displayed in Fig. 2 for $b = 1.09$ Å impact parameter in the diagonal direction. The potential energy along the red line (inset of Fig. 2) is lower than the reactant asymptote all along the path so that no activation energy is required for ER abstraction.

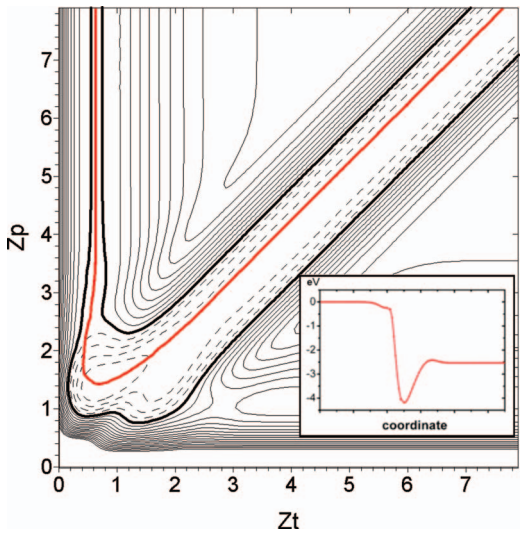

FIG. 2. 2D cut of the FPLEPS PES as a function of the altitude of both the target (Zt) and projectile (Zp) for $b = 1.09$ Å impact parameter in the diagonal direction. The thick black line indicates the zero energy level, taken as the N atomic adsorption energy. Full lines (dashed lines) are positive (negative) and separated by 0.8 eV. Inset: Variation of the potential along the red line. Distances are in Å.

QCT simulations have been performed in the following way. The adsorbate initially sits at its equilibrium position, i.e., at the center of the occupied cell with Zt = 0.65 Å above the surface. The 56 meV zero point energy of the nitrogen adatom (ZPE) is randomly shared between the 3 vibrational modes, i.e., the adsorbate initial momentum is randomly oriented. However, since the adsorption energy (7.37 eV) is high, initial dynamical conditions of the target (ZPE or no energy or Boltzmann distribution at surface temperature) have been found to negligibly influence the ER recombination dynamics. The projectile starts with normal incidence with respect to the surface from Zp = 8.0 Å altitude. Taking advantage of surface symmetry, the projectile initial coordinates (x, y) are uniformly selected in an octant of the unitary cell. Classical equations of motions are integrated using a velocity Verlet algorithm[99,100] with a $\Delta t = 0.121$ fs time step and collision energies are sampled within the range 0.1–3.0 eV. For each collision energy 30 000 trajectories are run.

The exit channels definition is inspired from the one employed by Martinazzo *et al.* in Ref. 53. Trajectories are integrated up to the projectile's first rebound, which is defined as a sign change in the z linear momentum. Then, the N–N distance is checked at each time step. If this distance gets larger than the maximum value ascribable to the N_2 diatomic molecule, R_{N_2}, the dynamical event is classified as HA formation. R_{N_2} is chosen large enough for the N–N interaction to be negligible with respect to the N–W(100) one. As a consequence, the total interaction energy reduces to the sum of two separated atom-surface interactions. In practice, the results presented below are insensitive to the value of R_{N_2} for $R_{N_2} \geq 2.5$ Å in the case of the rigid surface. Two HA channels are considered depending on the final energy of both N atoms. In the *metastable* HA process (mHA), the total energy

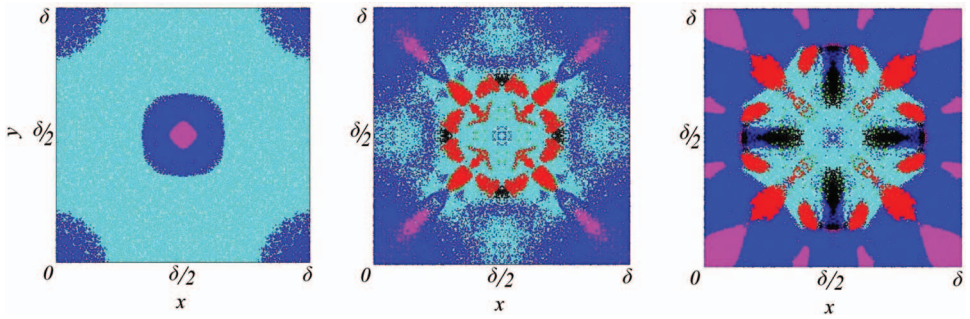

FIG. 3. Opacity maps of initial coordinates (x, y) of the projectile leading to the different exit channels: reflection (magenta dots), absorption (black dots), bound (cyan dots) and metastable (blue dots) HA formation, trapped molecules (green dots), and ER reactions (red dots) for 0.3 eV (left), 1.0 eV (center), and 2.6 eV (right) collision energy. The square represents the unitary cell in the center of which the nitrogen adatom is initially adsorbed. Distances are given in units of $\delta = 3.175$ Å.

of either nitrogen atom is greater than the minimum energy to escape from surface attraction whereas in the *bound* HA channel (bHA) both N atoms are trapped close to the surface. *Metastable* HA trajectories are further integrated and classified as direct reflection (REF) if they do not involve any additional rebound. The collision process is defined as *absorption* (ABS) if the z coordinate of any N atom gets lower than -0.5 Å, which corresponds to the minimal potential energy barrier to diffuse into the surface (over the bridge site). The Eley–Rideal recombination process is supposed to occur when the z coordinate of both atoms gets greater than the initial altitude of the projectile with positive N_2 center-of-mass momentum along z. It is also required that such a momentum only changes sign once along the entire trajectory. Otherwise, the process is classified as *trapped molecule formation* (TM). R_{N_2} is a critical parameter of the analysis so that we checked that the results presented in the following are insensitive to its particular value above 2.5 Å.

Simulations have been first performed within the rigid surface model. Then, to account for dissipation to phonons as well as temperature effects, a generalized Langevin oscillator model[101–104] has been used. In such a model the motion of surface atoms is described through a 3D harmonic oscillator coupled to a thermal bath to take into account the energy dissipated to the bulk. The mass associated with the surface oscillator is the W atomic mass (see Ref. 103 and references therein). The frequencies are chosen to represent the W(100) surface phonons. Following Ref. 105, we have checked that our results do not differ qualitatively when the frequencies associated with surface oscillators are modified by 2 orders of magnitude. Such a model has been found of reasonable validity for many gas-surface processes.[78,79,105–107]

III. RESULTS AND DISCUSSION

A. Rigid surface model

In this section, we focus on the N_2 ER recombination dynamics over a rigid W(100) surface. Nevertheless, part of the conclusions drawn within this approximation proves valid when energy transfers to the substrate are accounted for.

Figure 3 displays opacity maps, i.e., projections of the projectile's initial coordinates onto the surface unitary cell (x, y), in the center of which the N target is adsorbed for 0.3, 1.0, and 2.6 eV collision energies. As described in the caption, the color depends on the outcome for the collision following the definition of the reaction channels from Sec. II. As energy exchange with the surface is ignored so far, *bound* hot atoms are formed by transferring all initial collision energy to the target. In the opposite case, *metastable* hot atoms are created, which eventually desorb.

At 0.3 eV collision energy—Fig. 3 (left)—the dynamics is dominated by *bound* HA formation (cyan). However, *metastable* HA (blue) are created due to direct impact over the top tungsten atoms (4 corners) and over the target (center of the occupied cell). Reflections (magenta) about the target also appear, as a consequence of the potential energy bump revealed in Fig. 1. Notice the absence of ER reactions (red) at such low collision energies. At 1.0 eV—Fig. 3 (center)—the reflections and HA formations initiated with impact parameters close to the adsorbate disappear. The relative importance of *bound* HA (cyan) formation decreases with respect to the *metastable* HA (blue) channel. ER reactions now take place for low impact parameter ($b < 1.5$ Å). At 2.6 eV collision energy—Fig. 3 (right)—the *bound* HAs (cyan) only result from impact close to the center of the occupied cell and some collisions lead to direct absorption (black). The cross sections for the different outcomes for the collision are presented in Fig. 4 (notice the different scale for left and right plots).

The ER probability is very low compared to the probability for HA formations, in good agreement with previous results for hydrogen recombination on metals.[50,53] On the spanned collision energy range, the cross sections for ER and HA formation are lower than 0.4 Å^2 and higher than 8.0 Å^2, respectively. The *metastable* HA formation cross section increases—while the one for *bound* HA decreases—as projectile's collision energy increases. This stems from the fact that the proportion of energy transferred to the target decreases while projectile's velocity increases thus lowering *bound* HA formation at the expense of *metastable* HA formation. Absorption and reflection increase with increasing collision energy while trapped molecular formation remains low and approximately constant over the whole energy range.

The ER recombination cross section increases monotonously with collision energy above the 0.53 eV

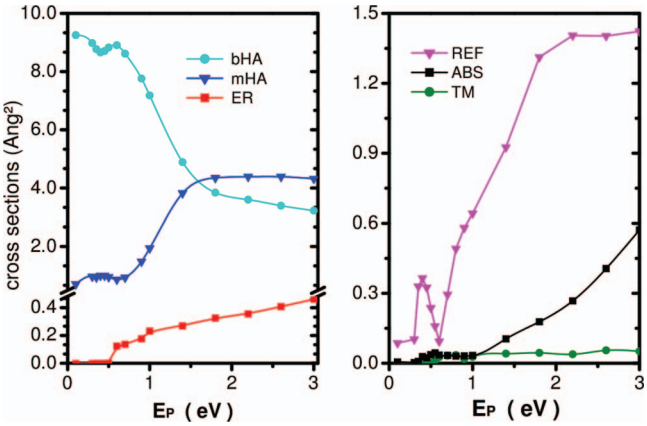

FIG. 4. Left: Cross sections for bound (bHA, circles), metastable (mHA, triangles) HA formation and ER reaction (squares). Right: Cross sections for trapped molecule formation (TM, circles), reflection (REF, triangles) and absorption (ABS, squares) as a function of the projectile energy.

threshold. As can be seen from the opacity maps of Fig. 3 (red patterns), the impact parameters which lead to reaction get larger with collision energy. ER recombination can be divided into two contributions depending on the dynamics of the abstraction process. ER1 contribution corresponds to reactions for which the projectile motion is approximately restricted to the above-mentioned diagonal plane in the reactant channel (or the one cutting the two other corners of the unit cell, equivalent by symmetry). ER2 process involves more intricate out-of-plane dynamics. For 1.9 eV collision energy, both contributions are presented in the opacity map of Fig. 5 (left). Their respective cross section as a function of collision energy (right) is also displayed. As evidenced in the figure, ER1 and ER2 reactions exhibit the same 0.53 eV threshold. ER2 contribution rises rapidly after threshold and is then almost constant, oscillating around 0.15 Å^2. The shape of the total ER reaction cross section is thus mainly governed by the ER1 contribution which increases monotonously with collision energy beyond threshold.

The (x, y) position of the target and projectile (at first projectile's rebound) as well as their altitude distribution are presented in Fig. 6 (top) for the ER1 mechanism. The corresponding initial conditions are presented in Fig. 5 (left). The dynamics of ER1 contribution is rather simple: during the vertical descent, projectiles are laterally deflected by the potential bump above the adsorbate (Zp $\sim$ 2.5–3.0 Å, see also Fig. 1) towards the top tungsten atoms on which they bounce (around Zp $\sim$ 1.0 Å) being thus reoriented towards the center of the cell. The projectile bounces at an altitude higher than that of the target (see Fig. 6, right) and thus picks it up from the above. The dynamics of the ER2 recombinations is more difficult to rationalize, as the motion of the projectile involves out-of-plane dynamics. Typically, the projectile moves down to the surface making a turn (in xy plane) while being redirected towards the center of the occupied cell, where the reaction takes place. In that case the target is picked up from below by the projectile (see Fig. 6, right). For all ER contributions, the molecule is formed immediately after the first projectile's rebound and quickly escape to the gas phase. Over the energy range considered here, the average time spent in the strong coupling region is of the order of 0.1 ps and does not vary drastically with collision energy.

The absence of ER recombination below 0.53 eV is the consequence of N–N repulsion in the entrance channel: after deflection by the potential energy bump, the N projectile needs to be redirected towards the center of the cell to trigger abstraction. Such redirection dynamics governs recombination. Figure 7 displays the projections of relevant ER1 trajectories onto the 2D cut of the PES. Impact parameters are uniformly sampled and trajectories are integrated from Zp = 8.0 Å down to the first rebound of the projectile. Three collision energies are considered: 0.1 eV (top), 0.5 eV (middle), and 0.6 eV (bottom). Below threshold, 0.1 and 0.5 eV, low impact parameter collisions (between 0 and 0.4 Å) are directly reflected by the potential energy bump "protecting" the adsorbate. Collisions initiated at larger impact parameters (between 0.4 and 2.2 Å) are deflected towards the top W atoms.

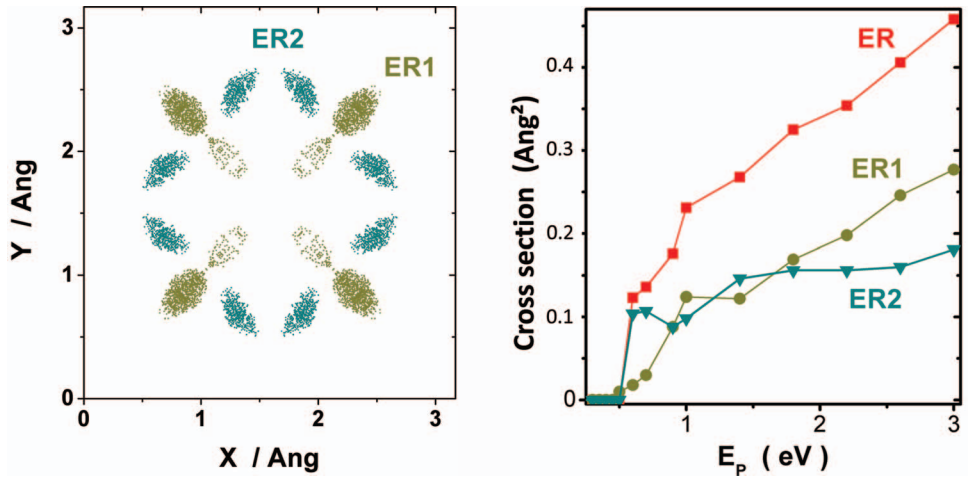

FIG. 5. Eley–Rideal contributions. Left: Opacity map of initial coordinates (x, y) of the projectile leading to ER1 (dark yellow dots), located along the diagonal, and ER2 (dark cyan dots). The square represents the unitary cell. Right: Eley–Rideal recombination cross section (squares) decomposed in its ER1 (circles) and ER2 (triangles) contributions as a function of projectile energy.

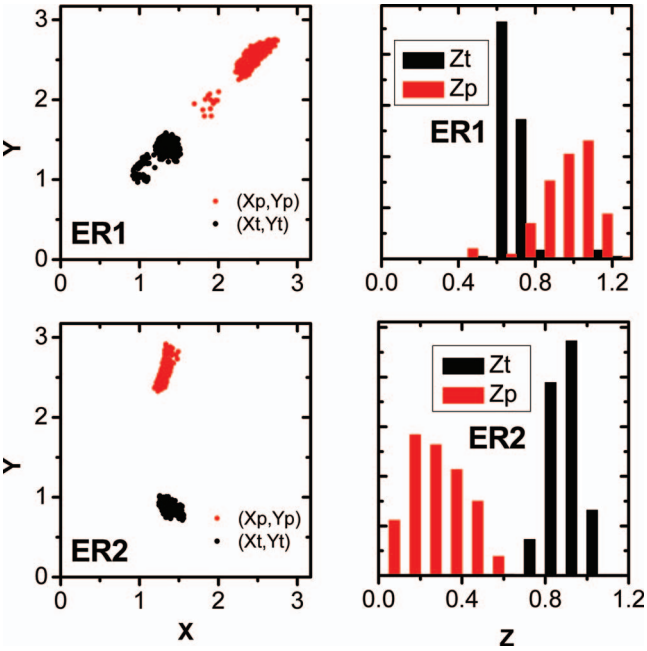

FIG. 6. Opacity map of (x, y) positions of the target and projectile (left) and their altitude distribution (right) at first projectile's rebound for the ER1 (up) and ER2 (bottom) mechanisms. Projectile (target) contribution is displayed in color red (black). Distances are in Å.

As inferred from the figure, the repulsive wall on which the projectile bounces, at the limit of the unit cell, reflects it back to the vacuum or towards the empty neighboring cell. Such reflection might thus trigger HA reactions for finite coverage. As the energy of the projectiles increases, the proportion of trajectories reflecting on the potential bump decreases and the deviation from the z-rectilinear propagation gets smaller. At 0.6 eV, small impact parameter projectiles bounce on a repulsive wall which redirects it towards the center of the unitary cell, thus triggering ER recombination (in red in the figure). Such a picture is only qualitative, as the target is slightly displaced during the projectile approach as shown in Fig. 6. It has to be noticed that preliminary results for off-normal incidence (30° and 45° with respect to surface normal) exhibit threshold to ER abstraction and opacity maps display patterns similar to the one of Fig. 6. The influence of the entrance potential energy bump is thus expected to play a non-negligible role whatever the collision incidence. In a complementary study,[108] a similar methodology was used to analyze the dynamics of molecular recombination upon impact on the neighboring empty cells. The computed ER cross section is almost zero ($\sim 1 \times 10^{-3}$ Å^2), indicating that the influence of the adsorbed nitrogen atom is negligible outside the occupied cell. A similar behavior is observed in the H+H/Ni(100) system, studied by Martinazo *et al.*[53]

It is worth noticing that N_2 ER recombinations involve a collision with the W surface prior to reaction, as already observed for H_2 and HCl recombination on metals.[63,109] Consequently, as the N/W mass ratio (0.076) is appreciable, potential energy transfers to the phonons during recombination might be of importance. This issue is considered in Sec. III B.

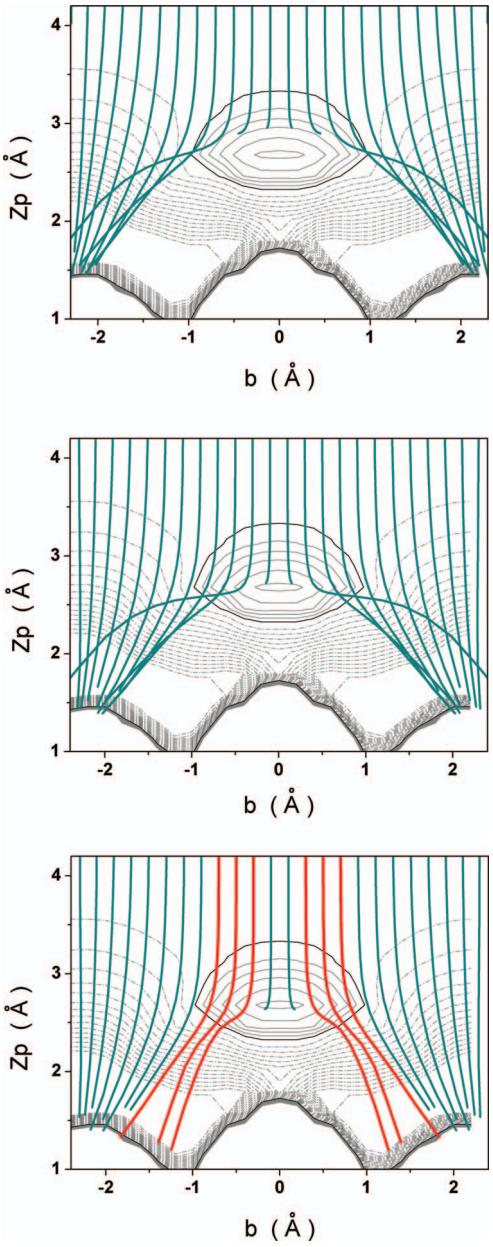

FIG. 7. Overlapping of trajectories on the 2D representation of the PES of Fig. 1 for different collision energies: 0.1 eV (top), 0.5 eV (middle), and 0.6 eV (bottom). Impact parameters are uniformly sampled within the diagonal plane. All trajectories are integrated until the first bounce. Trajectories in red indicate the zones where ER reactions take place.

B. Moving surface model

Possible energy transfers to the metal, which have been neglected so far, are accounted for within the framework of the generalized Langevin oscillator model. Figure 8 displays opacity maps for 1.0 eV (upper figures) and 2.6 eV (lower figures) collision energies and three surface temperatures : 300 K (left), 800 K (center), and 1500 K (right). The N adatom ZPE is accounted for but, as in the rigid surface case, the dynamical initial conditions for the target negligibly influence the abstraction dynamics.

The comparison of Fig. 8 (left column) with its rigid-surface counterpart (Fig. 3) reveals that the inclusion of the energy dissipation to the substrate changes the ER

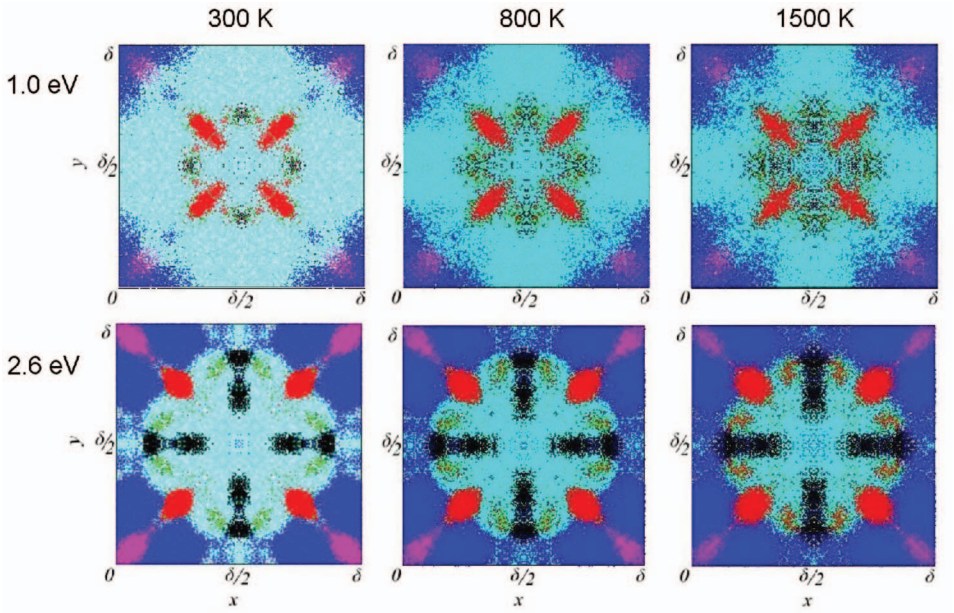

FIG. 8. Opacity maps of initial coordinates (x; y) of the projectile leading to the different exit channels: reflection (magenta dots), absorption (black dots), bound (cyan dots) and metastable (blue dots) HA formation, trapped molecules (green dots), and ER reactions (red dots) at different energies—1.0 eV (upper figures) and 2.6 eV (lower figures)—and temperatures: 300 K (left), 800 K (center), and 1500 K (right). The square represents the unitary cell the center of which the Nitrogen adatom is initially adsorbed. Distances are given in units of $\delta = 3.175$ Å.

recombination dynamics. ER2 component is mainly converted into trapped molecule formation (green). This latter contribution results from intricate dynamics close to the surface which induces multiple center-of-mass rebound for the forming molecule. Consistently, reflections are less probable and bound HA contribution increases as energy exchange upon collision of the projectile with the surface are allowed (not shown). When the temperature increases, the well defined patterns observed within the framework of the rigid-surface (Fig. 3) become blurred. As in the rigid-surface case, the formation cross section of metastable hot atoms increases—while the formation cross section of bound HA decreases—with the initial kinetic energy of projectiles. The direct absorption is clearly favored by the surface motion, especially at high energies.

In Fig. 9, the calculated ER abstraction cross section at various temperature is compared with the rigid-surface results. The ER cross section significantly decreases when surface motion is accounted for. As suggested before, this is the consequence of the disappearance of ER2 contribution (compare Figs. 3 and 8). A very slight increase of the ER cross section is observed when temperature increases from 300 K to 1500 K (see Fig. 9). On the opposite, the cross section for bound HA formation decreases with temperature (the cyan contribution decreases from left to right in Fig. 8). At low temperatures, the surface only receive energy from the nitrogen atoms, leading to a maximum dissipation to the substrate. When surface temperature increases, exchange of energy between nitrogen and tungsten atoms is lower and takes place in both directions: if surface temperature is high enough, reactant nitrogen atoms may even receive energy from the metal before being reflected back towards the vacuum. The detailed study of energy exchanges upon N_2 Eley–Rideal recombination is currently underway.[110]

To summarize, our results suggest that ER abstraction dynamics of N-pre-adsorbed atoms on W(100) by atomic nitrogen is essentially governed by the entrance channel N–N repulsion associated with the strong attraction of the projectile towards the top W surface atoms. Impinging atoms are radially deflected upon adatom approach and bounce on the nearest W top atoms prior to abstraction, thus strongly reflecting the symmetry of the metal surface. Investigations to evaluate the influence of surface symmetry on ER abstraction dynamics are currently underway.

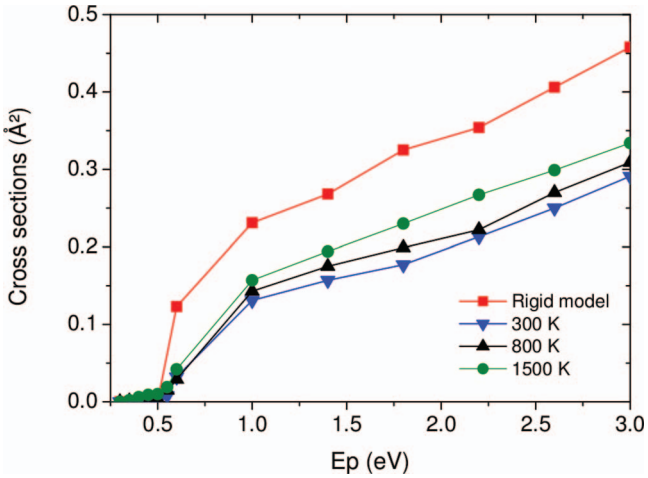

FIG. 9. Cross section for ER abstraction within the rigid surface model and the moving surface model at T_s = 300, 800, and 1500 K as a function of collision energy.

IV. CONCLUSIONS

Classical dynamics simulations of the normal scattering of atomic nitrogen off a N-pre-adsorbed W(100) are presented in the zero coverage limit. The adiabatic ground state potential energy surface, which has been recently developed, accurately reproduces the topology of the interactions. The ER abstraction and *hot atom formation* processes are analyzed both in the cases of rigid and moving surfaces. Energy transfers to the surface as well as temperature effects are accounted for using a generalized Langevin oscillator model. In the investigated collision energy range (0.1–3.0 eV), *hot atom formation*—by energy transfer to the target or the surface—is more than one order of magnitude more probable than ER recombination. Such a result is similar to what is observed for ER Hydrogen recombination on metal surfaces. A significant 0.53 eV collision energy threshold is found for ER abstraction despite the existence of non-activated reaction pathways. Such a feature, which to our knowledge has not been reported in ER recombination of diatomic molecule from metal surfaces, results from an interplay between entrance channel N–N repulsion and the strong attraction of the projectile towards the top W surface atoms which governs low energy dynamics. The effect of surface temperature on ER cross section is relatively minor.

ACKNOWLEDGMENTS

The authors acknowledge R. Diez-Muino, M. Alducin, and A. Cadi for rewarding discussions and advices on density functional theory computations. E.Q.S. acknowledges the Bordeaux1-InSTEC inter university agreement and the French embassy in Cuba for fundings.

[1]M. J. Molina, L. T. Molina, and D. M. Golden, "Environmental chemistry (gas and gas-solid interactions): The role of physical chemistry," J. Phys. Chem. **100**, 12888–12896 (1996).
[2]J. M. Greenberg, "Cosmic dust and our origins," Surf. Sci. **500**, 793–822 (2002).
[3]G. Winnewisser and E. Herbst, "Interstellar molecules," Pep. Prog. Phys. **56**, 1209–1273 (1993).
[4]J. S. Mathis, "Observations and theories of interstellar dust," Pep. Prog. Phys. **56**, 605–652 (1993).
[5]*Molecular Physics and Hypersonic Flows*, edited by M. Capitteli, NATO ASI Series C Vol. 482 (Kluwer Academic, Dordrecht, 1989).
[6]G. Federici, P. Andrew, P. Barabaschi, J. Brooks, R. Doerner, A. Geier, A. Herrmann, G. Janeschitz, K. Krieger, A. Kukushkin, A. Loarte, R. Neu, G. Saibene, M. Shimada, G. Strohmayer, and M. Sugihara, "Key ITER plasma edge and plasma–material interaction issues," J. Nucl. Mater. **313**, 11–22 (2003).
[7]A. W. Kleyn, N. J. L. Cardozo, and U. Samm, "Plasma–surface interaction in the context of ITER," Phys. Chem. Chem. Phys. **8**, 1761–1774 (2006).
[8]T. Rayment, R. Schlögl, J. M. Thomas, and G. Ertl, "Structure of the ammonia synthesis catalyst," Nature (London) **315**, 311–313 (1985).
[9]G. A. Somorjai, *Introduction to Surface Chemistry and Catalysis* (Wiley, New York, 1994).
[10]K. Honkala, A. Hellman, I. Remediakis, A. Logadottir, A. Carlsson, S. Dahl, C. Christensen, and J. Norskov, "Ammonia synthesis from first-principles calculations," Science **307**, 555–558 (2005).
[11]G. D. Billing, *Molecule Surface Interactions* (Wiley, New York, 2000).
[12]P. W. Tamm and L. D. Smith, "Crystallographic anisotropies in condensation: N_2 on (110) W," Surf. Sci. **26**, 286–296 (1971).
[13]S. W. Singh-Boparail, M. Bowker, and D. A. King, "Crystallographic anisotropy in chemisorption: Nitrogen on tungsten single crystal planes," Surf. Sci. **53**, 55–73 (1975).
[14]A. Kara and A. E. DePristo, "On the concept and distribution of reactive sites in dissociative chemisorption," J. Chem. Phys. **92**, 5653–5660 (1990).
[15]G. Volpilhac, H. F. Busnengo, W. Dong, and A. Salin, "Scattering of atomic nitrogen on W(100)," Surf. Sci. **544**, 329–338 (2003).
[16]G. Volpilhac and A. Salin, "Dissociative adsorption of N_2 on the W(100) surface," Surf. Sci. **556**, 129–144 (2004).
[17]M. Alducin, R. Díez-Muiño, H. F. Busnengo, and A. Salin, "Why N_2 molecules with thermal energy abundantly dissociate on w(100) and not on w(110)," Phys. Rev. Lett. **97**, 056102 (2006).
[18]M. Alducin, R. Díez-Muiño, H. F. Busnengo, and A. Salin, "Low sticking probability in the nonactivated dissociation of N_2 molecules on W(110)," J. Chem. Phys. **125**, 144705 (2006).
[19]M. Alducin, R. Díez, H. F. Busnengo, and A. Salin, "Dissociative adsorption of N_2 on W(110): Theoretical study of the dependence on the incidence angle," Surf. Sci. **601**, 3726–3730 (2007).
[20]G. A. Bocan, R. Díez, M. Alducin, and H. F. Busnengo, "The role of exchange-correlation functionals in the potential energy surface and dynamics of N_2 dissociation on W surfaces," J. Chem. Phys. **128**, 154704 (2008).
[21]L. Martin-Gondre, C. Crespos, P. Larrégaray, J-C. Rayez, B. van Ootegem, and D. Conte, "Is the leps potential accurate enough to investigate the dissociation of diatomic molecules on surfaces?" Chem. Phys. Lett. **471**, 136–142 (2009).
[22]L. Martin-Gondre, C. Crespos, P. Larrégaray, J-C. Rayez, B. van Ootegem, and D. Conte, "Dynamics simulation of N_2 scattering onto W(100,110) surfaces: A stringent test for the recently developed flexible periodic London–Eyring–Polanyi–Sato potential energy surface," J. Chem. Phys. **132**, 204501 (2010).
[23]L. Martin-Gondre, C. Crespos, P. Larrégaray, J-C. Rayez, D. Conte, and B. van Ootegem, "Detailed description of the flexible periodic London–Eyring–Polanyi–Sato potential energy function," Chem. Phys. **367**, 136–147 (2010).
[24]H. E. Pfnür, C. T. Rettner, J. Lee, R. J. Madix, and D. J. Auerbach, "Dynamics of the activated dissociative chemisorption of N_2 on W(110): A molecular beam study," J. Chem. Phys. **85**, 7452–7466 (1986).
[25]C. T. Rettner, E. K. Schweizer, H. Stein, and D. J. Auerbach, "Role of surface temperature in the precursor-mediated dissociative chemisorption of N_2 on W(100)," Phys. Rev. Lett **61**, 986–989 (1988).
[26]C. T. Rettner, H. Stein, and E. K. Schweizer, "Effect of collision energy and incidence angle on the precursor-mediated dissociative chemisorption of N_2 on W(100)," J. Chem. Phys. **89**, 3337–3341 (1988).
[27]C. T. Rettner, E. K. Schewizer, and H. Stein, "Dynamics of the chemisorption of N_2 on W(100): Precursor mediated and activated dissociation," J. Chem. Phys. **93**, 1442 (1990).
[28]M. Beutl, K. D. Rendulic, and G. R. Castro, "Does the rotational state of a molecule influence trapping in a precursor? An investigation of N_2/W(100), Co/FeSi(100) and O_2/Ni(111)," Surf. Sci. **385**, 97–106 (1997).
[29]W. Bohmeyer, F. L. Tabarés, M. Baudach, A. Cwiklinski, A. Markin, T. Schwarz-Selinger, J. A. Ferreira, G. Fussmann, and A. Loarte, "The scavenger effect – does it work?" J. Nucl. Mater. **390–391**, 560–563 (2009).
[30]F. L. Tabarés, J. A. Ferreira, A. Ramos, G. van Rooij, J. Westerhout, R. Al, J. Rapp, A. Drenik, and M Mozetic, "Suppression of tritium retention in remote areas of ITER by nonperturbative reactive gas injection," Phys. Rev. Lett. **105**, 175006 (2010).
[31]H. Umemoto, T. Funae, and Y. A. Mankelevich, "Activation and decomposition of N_2 on heated tungsten filament surfaces," J. Phys. Chem. C **115**, 6748–6756 (2011).
[32]K. W. Kolasinski, *Surface Science* (Wiley, New York, 2002).
[33]W. H. Weinberg, "Kinetics of surface reactions," in *Dynamics of Gas Surface Interactions*, edited by C. T. Rettner, and M. N. R. Ashfold (Royal Society of Chemistry, London, 1991), pp. 171–219.
[34]B. Halpern and D. E. Rosner, "Chemical energy accommodation al catalyst surfaces," J. Chem. Soc., Faraday Trans. **74**, 1883–1912 (1978).
[35]D. D. Eley and E. K. Rideal, "Parahydrogen conversion on tungsten," Nature (London) **146**, 401–402 (1940).
[36]D. D. Eley and E. K. Rideal, "The catalysis of the parahydrogen conversion by tungsten," Proc. R. Soc. London, Ser. A **178**, 429–451 (1941).
[37]D. D. Eley, "The interchange of hydrogen in the adsorbed film on tungsten," Proc. R. Soc. London, Ser. A **178**, 452–464 (1941).
[38]C. T. Rettner, "Dynamics of the direct reaction of hydrogen atoms adsorbed on Cu(111) with hydrogen atoms incident from the gas phase," Phys. Rev. Lett. **69**, 383–386 (1992).

[39]C. T. Rettner, "Reaction of an H atom beam with Cl/Au(111): Dynamics of concurrent Eley–Rideal and Langmuir–Hinshelwood mechanisms," J. Chem. Phys. **101**, 1529–1546 (1994).
[40]C. T. Rettner, H. A. Michelsen, and D. J. Auerbach, "Quantum-state-specific dynamics of the dissociative adsorption and associative desorption of H_2 at a Cu(111) surface," J. Chem. Phys. **102**, 4625–4641 (1995).
[41]B. Jackson and M. Persson, "A quantum mechanical study of recombinative desorption of atomic hydrogen on a metal surface," J. Chem. Phys. **96**, 2378–2387 (1992).
[42]M. Persson and B. Jackson, "Flat surface study of the Eley–Rideal dynamics of recombinative desorption of hydrogen on a metal surface," J. Chem. Phys. **102**, 1078–1093 (1995).
[43]B. Jackson and M. Persson, "Effects of isotopic substitution on Eley–Rideal reactions and adsorbate-mediated trapping," J. Chem. Phys. **103**, 6257–6279 (1995).
[44]S. Caratzoulas, B. Jackson, and M. Persson, "Eley–Rideal and hot-atom reaction dynamics of H(g) with H adsorbed on Cu(111)," J. Chem. Phys. **107**, 6420–6431 (1997).
[45]D. V. Shalashilin and B. Jackson, "Formation and dynamics of hot-precursor hydrogen atoms on metal surfaces: Trajectory simulations and stochastic models," J. Chem. Phys. **109**, 2856–2865 (1998).
[46]D. V. Shalashilin, B. Jackson, and M. Persson, "Eley–Rideal and hot-atom dynamics of HD formation by H(D) incident from the gas phase on D(H)-covered Cu(111)," Faraday Discuss. **110**, 287–300 (1998).
[47]C. Kalyanaraman, D. Lemoine, and B. Jackson, "Eley–Rideal and hot-atom reactions between hydrogen atoms on metals: Quantum mechanical studies," Phys. Chem. Chem. Phys. **1**, 1351–1358 (1999).
[48]D. V. Shalashilin, B. Jackson, and M. Persson, "Eley–Rideal and hot-atom reactions of H(D) atoms with D(H)-covered Cu(111) surfaces: Quasiclassical studies," J. Chem. Phys. **110**, 11038–11046 (1999).
[49]B. Jackson and D. Lemoine, "Eley–Rideal reactions between H atoms on metal and graphite surfaces: The variation of reactivity with substrate," J. Chem. Phys. **114**, 474–482 (2001).
[50]Z. B. Guvenc, X. Sha, and B. Jackson, "Eley–Rideal and hot atom reactions between hydrogen atoms on Ni(100): Electronic structure and quasiclassical studies," J. Chem. Phys. **115**, 9018–9027 (2001).
[51]Z. B. Guvenc, X. Sha, and B. Jackson, "The effects of lattice motion on Eley-Rideal and hot atom reactions: Quasiclassical studies of hydrogen recombination on Ni(100)," J. Phys. Chem. B **106**, 8342–8348 (2002).
[52]Z. B. Guvenc and D. Guvenc, "Hydrogen recombination on a mixed adsorption layer at saturation on a metal surface: H → (D+H)sat + Ni(100)," Surf. Sci. **529**, 11–22 (2003).
[53]R. Martinazzo, S. Assoni, G. Marinoni, and G. F. Tantardini, "Hot-atom versus Eley–Rideal dynamics in hydrogen recombination on Ni(100). I. The single-adsorbate case," J. Chem. Phys. **120**, 8761–8771 (2004).
[54]G. Lanzani, R. Martinazzo, G. Materzanini, I. Pino, and G. F. Tantardini, "Chemistry at surfaces: From *ab initio* structures to quantum dynamics," Theor. Chem. Acc. **117**, 805–825 (2007).
[55]J. Harris and B. Kasemo, "On precursor mechanisms for surface reactions," Surf. Sci. **105**, L281–L287 (1981).
[56]B. Jackson, X. Sha, and Z. B. Guvenc, "Kinetic model for Eley–Rideal and hot atom reactions between H atoms on metal surfaces," J. Chem. Phys. **116**, 2599–2608 (2002).
[57]H.-J. Ernst, E. Hulpke, and J. P. Toennies, Phys. Rev. B **46**, 16081 (1992).
[58]S. Titmuss, A. Wander, and D. A. King, Chem. Rev. **96**, 1291 (1996).
[59]H. F. Busnengo and A. E. Martinez, J. Phys. Chem. C **112**, 5579–5588 (2008).
[60]C. Díaz, J. K. Vincent, G. P. Krishnamohan, R. A. Olsen, G. J. Kroes, K. Honkala, and J. K. Norskov, "Multidimensional effects on dissociation of N_2 on Ru(0001)," Phys. Rev. Lett. **96**, 096102 (2006).
[61]G. J. Kroes, "Frontiers in surface scattering simulations," Science **321**, 794–797 (2008).
[62]J. G. Quattrucci, B. Jackson, and D. Lemoine, "Eley–Rideal reactions of H atoms with Cl adsorbed on Au(111): Quantum and quasiclassical studies," J. Chem. Phys. **118**, 2357–2365 (2003).
[63]D. Lemoine, J. D. Quattrucci, and B. Jackson, "Efficient Eley-Rideal reactions of H atoms with single Cl adsorbates on Au(111)," Phys. Rev. Lett. **89**, 268302 (2002).
[64]M. Persson and B. Jackson, "Isotope effects in the Eley-Rideal dynamics of the recombinative desorption of hydrogen on a metal surface," Chem. Phys. Lett. **237**, 468–473 (1995).
[65]S. Morisset, A. Aguillon, M. Sizun, and V. Sidis, "Quantum wavepacket investigation of Eley Rideal formation of H_2 on a relaxing graphite surface," Chem. Phys. Lett. **378**, 615–621 (2003).
[66]S. Morisset, A. Aguillon, M. Sizun, and V. Sidis, "Role of surface relaxation in the Eley-Rideal formation of H_2 on a graphite surface," J. Phys. Chem. A **108**, 8571–8579 (2004).
[67]S. Morisset, A. Aguillon, M. Sizun, and V. Sidis, "Quantum dynamics of H_2 formation on a graphite surface through the Langmuir hinshelwood mechanism," J. Chem. Phys. **121**, 6493–6501 (2004).
[68]S. Morisset and A. Allouche, "Quantum dynamic of sticking of a H atom on a graphite surface," J. Chem. Phys. **129**, 1–8 (2008).
[69]S. Morisset, Y. Ferro, and A. Allouche, "Isotopic effects in the sticking of H and D atoms on the (0001) graphite surface," Chem. Phys. Lett. **447**, 225–229 (2009).
[70]S. Morisset, Y. Ferro, and A. Allouche, "Study of the sticking of a hydrogen atom on a graphite surface using a mixed classical-quantum dynamics method," J. Chem. Phys. **133**, 1–10 (2010).
[71]S. Cazaux, S. Morisset, M. Spaans, and A. Allouche, "When sticking influences H_2 formation," Astron. Astrophys. **535**, 1–10 (2011).
[72]D. Bachellerie, M. Sizun, A. Aguillon, D. Teillet-Billy, N. Rougeau, and V. Sidis, "Unrestricted study of the Eley-Rrideal formation of H_2 on graphene using a new multidimensional graphene–H–H potential: Role of the substrate," Phys. Chem. Chem. Phys. **11**, 2715–2729 (2009).
[73]M. Sizun, D. Bachellerie, A. Aguillon, and V. Sidis, "Investigation of zpe and temperature effects on the Eley–Rideal recombination of hydrogen atoms on graphene using a multidimensional graphene–H–H potential," Chem. Phys. Lett. **498**, 32–37 (2010).
[74]I. Goikoetxea, J. I. Juaristi, M. Alducin, and R. Diez, "Dissipative effects in the dynamics of N_2 on tungsten surfaces," J. Phys. Condens. Matter **21**, 1–6 (2009).
[75]J. I. Juaristi, M. Alducin, R. Diez, H. F. Busnengo, and A. Salin, "Role of electron-hole pair excitations in the dissociative adsorption of diatomic molecules on metal surfaces," Phys. Rev. Lett. **100**, 116102 (2008).
[76]J. I. Juaristi, M. Alducin, R. Diez-Muino, H. F. Busnengo, and A. Salin, "Reply to comment on "Role of electron-hole pair excitations in the dissociative adsorption of diatomic molecules on metal surfaces"," Phys. Rev. Lett. **102**, 109602 (2009).
[77]A. C. Luntz, I. Makkonen, M. Persson, S. Holloway, D. M. Bird, and M. S. Mizielinski, "Comment on "role of electron-hole pair excitations in the dissociative adsorption of diatomic molecules on metal surfaces"," Phys. Rev. Lett. **102**, 109601 (2009).
[78]L. Martin-Gondre, M. Alducin, G. A. Bocan, R. Díez-Muiño, and J. I. Juaristi, "Competition between electron and phonon excitations in the scattering of nitrogen atoms and molecules off tungsten and silver metal surfaces," Phys. Rev. Lett. **108**, 096101 (2012).
[79]L. Martin-Gondre, G. A. Bocan, M. Alducin, J. I. Juaristi, and R. Díez-Muiño, "Energy dissipation channels in the adsorption of N on Ag(111)," Comput. Theor. Chem. **990**, 126–131 (2012).
[80]H. Nienhaus, "Electronic excitations by chemical reactions on metal surfaces," Surf. Sci. Rep. **45**, 1–78 (2002).
[81]P. Hohenberg and W. Kohn, "Inhomogeneous electron gas," Phys. Rev. **136**, B864 (1964).
[82]W. Kohn and L. J. Sham, "Self-consistent equations including exchange and correlation effects," Phys. Rev. **140**, A1133 (1965).
[83]A. D. Becke, "Density-functional exchange-energy approximation with correct asymptotic behavior," Phys. Rev. A **38**, 3098–3099 (1988).
[84]J. P. Perdew, "Density-functional approximation for the correlation energy of the inhomogeneous electron gas," Phys. Rev. B **33**, 8822–8824 (1986).
[85]W. Dong and J. Hafner, "H_2 dissociative adsorption on Pd(111)," Phys. Rev. B **56**, 15396–15403 (1997).
[86]A. Eichler, G. Kresse, and J. Hafner, "Quantum steering effects in the dissociative adsorption of H_2 on Rh(100)," Phys. Rev. Lett. **77**, 1119–1122 (1996).
[87]B. Hammer, M. Scheffler, and K. W. Jacobsen, "Multidimensional potential energy surface for H_2 dissociation over Cu(111)," Phys. Rev. Lett. **73**, 1400–1403 (1994).
[88]J. A. White, D. M. Bird, M. C. Payne, and I. Stich, "Surface corrugation in the dissociative adsorption of H_2 on Cu(100)," Phys. Rev. Lett. **73**, 1404–1407 (1994).
[89]G. Wiesenekker, G. J. Kroes, E. J. Baerends, and R. C. Mowrey, "Dissociation of H_2 on Cu(100): Dynamics on a new two-dimensional potential energy surface," J. Chem. Phys. **102**, 3873–3883 (1995).
[90]S. Wilke and M. Scheffler, "Poisoning of Pd (100) for the dissociation of H_2: A theoretical study of co-adsorption of hydrogen and sulphur," Surf. Sci. **329**, L605–L610 (1995).
[91]J. P. Perdew, J. A. Chevary, S. H. Vosko, K. A. Jackson, M. R. Pederson, D. J. Singh, and C. Fiolhais, "Atoms, molecules, solids, and surfaces:

Applications of the generalized gradient approximation for exchange and correlation," Phys. Rev. B **46**, 6671–6687 (1992).
[92]J. P. Perdew, J. A. Chevary, S. H. Vosko, K. A. Jackson, M. R. Pederson, D. J. Singh, and C. Fiolhais, "Erratum: Atoms, molecules, solids, and surfaces: Applications of the generalized gradient approximation for exchange and correlation [Phys. Rev. B 46, 6671 (1992)]," Phys. Rev. B **48**, 4978 (1993).
[93]J. P. Perdew, K. Burke, and Y. Wang, "Generalized gradient approximation for the exchange-correlation hole of a many-electron system," Phys. Rev. B **54**, 16533–16539 (1996).
[94]J. P. Perdew, K. Burke, and M. Ernzerhof, "Generalized gradient approximation made simple," Phys. Rev. Lett. **77**, 3865–3868 (1996).
[95]B. Hammer, L. B. Hansen, and J. K. Norskov, "Improved adsorption energetics within density-functional theory using revised Perdew-Burke-Ernzerhof functionals," Phys. Rev. B **59**, 7413–7421 (1999).
[96]D. Vanderbilt, "Soft self-consistent pseudopotentials in a generalized eigenvalue formalism," Phys. Rev. B **41**, 7892–7895 (1990).
[97]K. Laasonen, R. Car, C. Lee, and D. Vanderbilt, "Implementation of ultrasoft pseudopotentials in *ab initio* molecular dynamics," Phys. Rev. B **43**, 6796–6799 (1991).
[98]K. Laasonen, A. Pasquarello, R. Car, C. Lee, and D. Vanderbilt, "Car-parrinello molecular dynamics with Vanderbilt ultrasoft pseudopotentials," Phys. Rev. B **47**, 10142–10153 (1993).
[99]L. Verlet, "Computer "experiments" on classical fluids. I. Thermodynamical properties of Lennard-Jones molecules," Phys. Rev. **159**, 98–103 (1967).
[100]L. Verlet, "Computer "experiments" on classical fluids. II. Equilibrium correlation functions," Phys. Rev. **165**, 201–214 (1968).
[101]S. A. Adelman, "Generalized Langevin theory for many body problems in chemical dynamics: General formulation and the equivalent harmonic chain representation," J. Chem. Phys. **71**, 4471–4486 (1979).
[102]J. C. Polanyi and R. J. Wolf, "Dynamics of simple gas-surface interaction. II. Rotationally inelastic collisions at rigid and moving surfaces," J. Chem. Phys. **82**, 1555–1566 (1985).
[103]J. C. Tully, "Dynamics of gas-surface interactions: 3D generalized Langevin model applied to fcc and bcc surfaces," J. Chem. Phys. **73**, 1975–1985 (1980).
[104]M. Dohle, P. Saalfrank, and T. Uzer, "The dissociation of diatomic molecules on vibrating surfaces: A semiclassical generalized Langevin approach," J. Chem. Phys. **108**, 4226–4236 (1998).
[105]H. F. Busnengo, W. Dong, and A. Salin, "Trapping, molecular adsorption, and precursors for nonactivated chemisorption," Phys. Rev. Lett **93**, 236103 (2004).
[106]Y. Guan, J. T. Muckerman, and T. Uzer, "Desorption of vibrationally excited adsorbates in competition with relaxation: A classical picture," J. Chem. Phys. **93**, 4383–4399 (1990).
[107]H. F. Busnengo, M. A. Di Césare, W. Dong, and A. Salin, "Surface temperature effects in dynamic trapping mediated adsorption of light molecules on metal surfaces: H_2 on Pd(111) and Pd(110)," Phys. Rev. B **72**, 125411 (2005).
[108]L. Barrios-Herrera, E. Quintas-Sánchez, L. Martin-Gondre, C. Crespos, P. Larrégaray, J. Rubayo-Soneira, and J.-C. Rayez, "Sección eficaz Eley-Rideal en la recombinación de nitrógeno sobre tungsteno (100)," Rev. Cub. Fis. **28**, 61–65 (2011).
[109]B. Jackson and M. Persson, "Vibrational excitation in recombinative desorption of hydrogen on metal surfaces: Eley-Rideal mechanism," Surf. Sci. **269**, 195–200 (1992).
[110]E. Quintas-Sánchez, P. Larrégaray, C. Crespos, J.-C. Rayez, and J. Rubayo-Soneira (unpublished).